

Journal Pre-proofs

Synthesis and characterisation of polyurethane made from pyrolysis bio-oil of pine wood

Jaber Gharib, Shusheng Pang, Daniel Holland

PII: S0014-3057(20)30516-4

DOI: <https://doi.org/10.1016/j.eurpolymj.2020.109725>

Reference: EPJ 109725

To appear in: *European Polymer Journal*

Received Date: 4 March 2020

Revised Date: 24 April 2020

Accepted Date: 24 April 2020

Please cite this article as: Gharib, J., Pang, S., Holland, D., Synthesis and characterisation of polyurethane made from pyrolysis bio-oil of pine wood, *European Polymer Journal* (2020), doi: <https://doi.org/10.1016/j.eurpolymj.2020.109725>

This is a PDF file of an article that has undergone enhancements after acceptance, such as the addition of a cover page and metadata, and formatting for readability, but it is not yet the definitive version of record. This version will undergo additional copyediting, typesetting and review before it is published in its final form, but we are providing this version to give early visibility of the article. Please note that, during the production process, errors may be discovered which could affect the content, and all legal disclaimers that apply to the journal pertain.

© 2020 Published by Elsevier Ltd.



Synthesis and characterisation of polyurethane made from pyrolysis bio-oil of pine wood

Jaber Gharib, Shusheng Pang, Daniel Holland*

Department of Chemical and Process Engineering, University of Canterbury, Christchurch, New Zealand.

* Email: daniel.holland@canterbury.ac.nz

Abstract

This paper investigates the manufacture of polyurethane from pyrolysis bio-oil produced from radiata pine wood. Liquid-liquid extraction was used to separate bio-oil into fractions. These fractions were reacted with methylene diphenyl diisocyanate (MDI) to produce polyurethane. For comparison, a series of polyurethanes were prepared with castor oil in a similar manner. Among the various fractions of the bio-oil, the water-insoluble fraction (often referred to as pyrolytic lignin) was found to be the most appropriate component to produce polyurethane as it is a significant fraction of bio-oil and has a high hydroxyl number, hence, is able to produce a robust film. It was found that gradual addition of the polyol to MDI helped produce a more flexible and stable polyurethane film. Water absorption of bio-oil based polyurethane was found to be higher than that of castor oil based polyurethane. However, the diffusion coefficient of water in the bio-oil derived polyurethane was lower than in castor oil-derived polyurethane. These results suggest bio-oil derived polymers may be suitable for use as protective coatings.

1 Introduction

Polyurethane has many applications, so it is desirable to seek renewable sources to replace the petroleum-derived ingredients widely used today. Polyurethane represents a versatile class of polymeric materials [1], [2] in which repetitive structures are linked by carbamate (urethane). Synthesis of conventional polyurethane consists of the reaction between diisocyanates and polyols [3]. Polyols are defined as compounds with at least two hydroxyl (OH) groups which can continue the progress of the polymerisation chain. Depending on the type of polyol, the final product could be rigid or elastomeric [3]. Traditionally polyols were petroleum-based [4], but various vegetable oils have also been proposed [5]–[12]. Vegetable oils are often available locally, are friendly to the environment and in most cases are less expensive than petroleum-derived polyols. However, there are concerns that the resulting demand for these agricultural oils to produce polymers may compete with land needed for food production. It is therefore desirable to develop alternative polyols that are not derived from food crops nor use agricultural land. The purpose of this work is to investigate the viability of using bio-oil derived from pyrolysis of woody biomass as a polyol for the production of polyurethane films.

Bio-oil may be derived from the pyrolysis of waste wood residues, such as that produced when felling trees and processing logs for wood products, making it an economically attractive feedstock. Pyrolysis bio-oil is a thick liquid that is dark brown to black in colour and is rich in a large number of oxygenated compounds, though also contains 30-40 wt.% water [13]–[15]. Most of the chemicals in pyrolysis bio-oil fall into five broad families including hydroxyaldehydes, hydroxyketones, sugars and dehydrosugars, carboxylic acids, and phenolic compounds derived from lignin [16]. Hydroxyl structures can be found in sugars, alcohols, acids, furans and lignin derivatives [16]. Any of these species could potentially be used as polyols for the manufacture of polyurethane.

One barrier to using bio-oil as a polyol, is the complexity of the bio-oil. Although many species will contain hydroxyl groups, some do not and are unreactive with isocyanate. These components require separation and purification before bio-oil can be used to produce a polyurethane. It may be advantageous to include water if producing a polyurethane foam. However, for the production of protective films water must be removed from the polyol before reacting with the isocyanate

to avoid the formation of pores in the polyurethane [17]. Liquid-liquid extraction (LLE) is the most widely used approach to isolate the chemicals of pyrolysis bio-oil [18]. One of the most common LLE process is to fraction the bio-oil into water-soluble and water-insoluble compounds followed by washing water-insoluble and water-soluble fractions with dichloromethane and diethyl ether, respectively [19]–[22], though various other LLE approaches have also been proposed [23]–[26]. The ether-soluble fraction is claimed to be rich in aldehydes, ketones, phenols and furans. The ether-insoluble part contains mainly sugars. The water-insoluble fraction is primarily composed of species derived from lignin, many of which contain hydroxyl compounds. These species are sometimes split by DCM into low-molecular-mass (LMM) and high-molecular-mass (HMM) compounds in the DCM-soluble and DCM-insoluble fractions, respectively [22]. Since they are derived from lignin, they are collectively referred to as pyrolytic lignin. Pyrolytic lignin and the ether-insoluble fractions are promising candidates for production of polyurethane as they will contain multiple hydroxyl groups. Pyrolytic lignin can make up 15-30% of the bio-oil [27]–[29] and is typically regarded as a waste material in bio-oil processing for fuel, so this is the most promising fraction to use for manufacture of polyurethane.

Lignin, or more strictly kraft lignin or organosolv lignin, has often been proposed as a potential candidate for use as a polyol owing to the presence of several hydroxyl groups [30]–[35]. However, the high molecular weight and complex structure of lignin results in poor mixing with diisocyanates, significant steric hindrance and overall poor reactivity. Lignin is therefore mostly modified with various approaches such as oxidation, depolymerisation and oxypropylation before it can be used as a polyol [31]–[35]. Alternatively, lignin may be dissolved in other polyols such as castor oil, glycerol [36], cardanol [37], soybean oil [38], glycol (PEG) [39], [40] or molasses [41] to obtain a more desirable polyurethane. In all of these studies where untreated lignin was used, the lignin fraction was kept below 30% to ensure it is soluble [42] and the resulting polyurethane is not too brittle [43]. Using pretreatment processes, or limiting the content of lignin, make the manufacture of lignin based polyurethane uneconomic and/or unattractive. Recently, polyurethane coatings based on chemically unmodified lignin were obtained by fractionating lignin [44], suggesting an alternative method of incorporating lignin. Pyrolysis partially cracks lignin during the production of bio-oil. This pyrolytic lignin contains many of the

same functional groups as lignin, but the molecular weight distribution is shifted towards smaller molecules. The purpose of this study is to explore whether pyrolytic lignin can be used to manufacture polyurethane and to determine whether the resulting polyurethane is sufficiently ductile to be a useful polymer.

The mechanical properties of polyurethane are also affected by the process with which it is produced. In a one-step approach (one-shot), the ingredients are measured and homogeneously mixed simultaneously. Control of the structure of the chain and its development is difficult. Thus a two-step approach is often used. In the two-step approach, long-chain polyols are added to an excess amount of diisocyanate to form a prepolymer [45]. The prepolymer is reacted with a low molecular weight diol or a diamine as a chain extender. A soft section is made between the polyol and diisocyanate and a hard section between the chain extender and the diisocyanate [46], [47]. Therefore, good control of the mechanical properties of the polymer is possible by adjusting the type and proportion of chain extender in the final polymer. A similar approach can be used to reduce cross-linking of the final polymer, and hence improve its ductility [35].

In this study, bio-oil from pyrolysis of radiata pine wood chips was extracted into four fractions. The possibility of making polyurethane with each fraction was investigated. Here, pyrolytic lignin was used without any further modification. Different factors influencing the physical and mechanical properties of the polymers were determined. The thermal stability and water absorption of the polyurethane were then assessed. Polyurethane manufactured with castor oil in different ratios was also prepared to compare with the bio-oil-based polyurethanes.

2 Materials and Methods

2.1 Materials

Dichloromethane (DCM, 99.8% purity) was purchased from Lab-Scan. Diethyl ether (99.7% purity), acetone (99.9% purity) and tetrahydrofuran (THF, 99.9% purity) were all purchased from Sigma-Aldrich. Methylene diphenyl diisocyanate (MDI) (98% purity) was purchased from Aldrich and kept in the fridge to minimise the dimerization of the MDI. Castor oil was purchased from Sigma-Aldrich. Pyrolysis bio-oil was produced in-house from pine wood [48].

Karl Fischer (KF) titration was used to determine the water content. KF reagent HYDRANAL-composite 5 (Honeywell-Fluka®) was used, which consists of iodine, sulfur oxide, imidazole ($C_3N_2H_4$), 2-Methylimidazole ($CH_3C_3H_2N_2H$) and diethylene glycol monoethyl ether (DEGEE). Methanol causes an undesirable interference in the determination of water content [49], hence HYDRANAL Medium K (Honeywell-Fluka®) which is methanol free was used as the solvent for the polyols. HYDRANAL-water Standards (Fluka®) were used to standardize the KF titration.

The hydroxyl number was measured by reaction with phthalic anhydride using pyridine (99.9% purity), phthalic anhydride (99% purity), phenolphthalein and potassium hydrogen phthalate (KHP) (99.95% purity), all purchased from Sigma-Aldrich, and sodium hydroxide purchased from Ajax FineChem.

2.2 Methods

2.2.1 Liquid-Liquid Extraction

Bio-oil was produced from the pyrolysis of radiata pine. The bio-oil was stored for several months prior to liquid-liquid extraction. The bio-oil contained approximately 40% water at the time of this work, as measured by KF titration. The pyrolysis bio-oil was split into four fractions by liquid-liquid extraction. The bio-oil was first isolated into water-soluble and water-insoluble fractions (pyrolytic lignin) by adding water to bio-oil in the ratio of 2 parts water to 1 part bio-oil. The resulting two-phase mixture settled rapidly. The water-soluble fraction was decanted off the top. The water-soluble fraction was further fractionated by mixing with 150 g ether to extract ether-soluble and ether-insoluble fractions. The process produced 4 fractions of bio-oil from which polyurethane could be produced: (1) pyrolytic lignin (32 wt.%), (2) water-soluble (10 wt.%), (3) water-soluble and ether-soluble (2 wt.%), and (4) water-soluble and ether-insoluble (8 wt.%). The weight fractions were calculated after evaporation of the water and other volatile species and are relative to the original wet bio-oil mass. The remaining 18 wt.% of the bio-oil (in addition to water, the water-insoluble fraction and the water-soluble fraction) consisted of volatile species that were removed during drying.

2.2.2 Characterisation of polyols and Synthesis of Polyurethane

Prior to polyurethane production, the polyols were dried to < 0.2 wt.% water in a vacuum oven operating at $P = 4.3$ kPa (abs) and $T = 32^\circ\text{C}$. To avoid the sudden expansion of the polyol due to the evasion of trapped water, the temperature was increased gradually from room temperature to 32°C , which is 5°C above the boiling point of water at the operating absolute pressure. Later, KF titration (ASTM method E203) was used to measure the water content of the polyols. The method was implemented on a Mettler Toledo V10 Volumetric Titration system.

The hydroxyl number of polyols, H , was measured according to the ASTM standard [50]. However, as bio-oil is too dark for a colour change to be detected, a potentiometric measure of pH was used to determine the end point instead of the colour change. The hydroxyl number of castor oil, whole bio-oil and pyrolytic lignin were 163 ± 3 , 70 ± 4 and 57 ± 3 mg KOH/g sample, respectively.

Polymers were prepared with a defined ratio of isocyanate to hydroxyl groups, henceforth referred to as the NCO:OH ratio. The NCO:OH ratio was calculated from the functionality value of MDI and hydroxyl number of polyol as:

$$\text{NCO:OH ratio} = \frac{m_{\text{MDI}} M_{\text{KOH}} f_{\text{MDI}}}{m_{\text{polyol}} M_{\text{MDI}} H'} \quad (1)$$

where m_{MDI} is the mass of MDI (g), M_{MDI} is the molecular weight of MDI (g/mol), f_{MDI} is the functionality of MDI which was 2 mol NCO/mol MDI, m_{polyol} is the mass of polyol (g), H is the hydroxyl number of polyol (mg KOH/g), and M_{KOH} is the molecular weight of KOH (kg/mol).

Polyurethane films were manufactured using five methods, detailed in Table 1. Polyols and MDI were warmed to a pre-determined temperature for 5 minutes before mixing in an aluminum pan. In one shot method ingredients were added at once and mixed vigorously. In gradual methods, polyols were added dropwise to MDI at ~ 2 g/min. The polymers were spread on a microscope glass slide using a spatula just before the polymer was about to set (approximately 2 minutes). All polymers were left to solidify completely for 24 h. The polymers were then cured in an oven at atmospheric pressure and a temperature of 110°C for 4 h, unless otherwise stated. The final thickness of the polymers varied from 10-150 μm , depending on the specific preparation.

Table 1: Methods used to prepare polyurethane samples.

Method	Addition type	Sample size	Mixing Time	Polyol	T (°C)
Method 1	One-shot	~5 g	2	Castor oil	85
				R 0.75-11.3	95
					105
		~5 g	2	Bio-oil fractions	75
				Pyrolytic lignin	
				R 0.75, 1, 1.25, 1.5	
Method 2	Gradual	~5 g	2.5	Pyrolytic lignin	75
				R 0.75, 1, 1.25, 1.5	
Method 3	Gradual	~5 g	2.5	Pyrolytic lignin was mixed with MDI (R 1.3). This prepolymer was mixed with excess pyrolytic lignin to reach R 1.	75
Method 4	Gradual	~5 g	2.5	Pyrolytic lignin was mixed with MDI (R 1.3). This prepolymer was mixed with castor oil to reach R 1.	75
Method 5	Gradual	~5 g	2.5	Pyrolytic lignin was mixed with MDI (R 1.3). This prepolymer was mixed with castor oil to reach R 1.	75

2.2.3 Characterisation of Polyurethanes

The morphology of pyrolytic lignin-based and castor oil-based polyurethane films (both at NCO:OH ratio of 1) was investigated using an optical microscope (Nikon SMZ-1B) and scanning electron microscopy (SEM) (JEOL JSM IT-300 InTouchScope). For SEM, the polyurethane films were gold sputtered (Quorum EMS 150T ES) before scanning.

The degree of cross-linking (*DC*) was determined using the ASTM D2765-11 standard with some minor modifications. Polyurethane samples were moulded in the shape of a cuboid (26 mm along the sides, and 13 mm in thickness) and immersed in 50 ml of THF at room temperature for 24 h. Then the samples were removed from THF and dried in an oven at 110°C for 24 h to remove the solvents. The degree of cross-linking was calculated according to:

$$DC = \frac{m_2}{m_1}, \quad (2)$$

Where m_1 denotes the mass (g) of the polyurethane before immersing in THF and m_2 is the mass (g) of the polyurethane after drying.

Fourier Transform Infrared (FTIR) Spectroscopy was performed on each polyol, MDI and the resulting polyurethanes at room temperature using a Bruker IFS spectrometer to obtain the FTIR transmittance spectrum. Data were recorded over a wavelength range of 4000 to 400 cm^{-1} with a resolution of 4 cm^{-1} .

Thermal gravimetric analysis (TGA) of the polymers was performed using a NETZCH STA 449F3 instrument under a nitrogen atmosphere. Thermogravimetric data was collected from 30°C to 600°C with a heating rate of 5°C/min. Only 5 mg of each sample was used, to minimise the risk of the sample expanding out of the sample container at high temperatures.

The water absorption of polyurethane films was measured by immersing the specimens in water kept at 25°C in an oven. Each specimen included a layer of polyurethane (0.8-1.5 mm thick) which was spread on a glass microscope slide (20 mm by 70 mm). For each polyurethane, 3 samples were prepared and the absorption quantified from the average mass fraction absorbed by each sample. The samples were taken out of the water after 10 min, 1, 3, 5, 8, 10, 20, 40, 70 and 100 h. The samples were then pat-dried with a tissue to remove the surface water and weighed. The water absorbed (A) was calculated according to:

$$A = \frac{m_t - m_i}{m_i}, \quad (3)$$

where m_t denotes the mass of polyurethane at time t and m_i is the initial mass of polyurethane.

3 Results and discussion

In this section, visual observations of the polymers made from different ingredients, NCO:OH ratios and conditions are initially presented. The most promising polyols and polymerisation conditions were selected for further investigation. The films produced were studied using FTIR to identify the main reactive agents of the polyols and the characteristic structures of polyurethanes. The thermal stability of the polymers was determined using TGA. Water absorption was measured and used to estimate the diffusion coefficient of water in the polyurethane films.

3.1 Effect of preparation methods

Polyurethane prepared from bio-oil is opaque, making visual characterisation challenging. Therefore, initially polyurethanes of castor oil were synthesized. Figure 1 shows photographs of castor oil polyurethane films at NCO:OH ratios of 11.3, 4.2, 2.7, 1.5, 1 and 0.75 prepared at 85°C. At high NCO:OH ratios, the resulting polyurethane was brittle due to the presence of unreacted or partially reacted MDI. The polyurethane became malleable at NCO:OH ratios below 1.5. When the NCO:OH ratio decreased below 1, a sticky polymer resulted due to the presence of excess castor oil. An increase in the reaction temperature increased the reaction rate and hence rate of solidification.

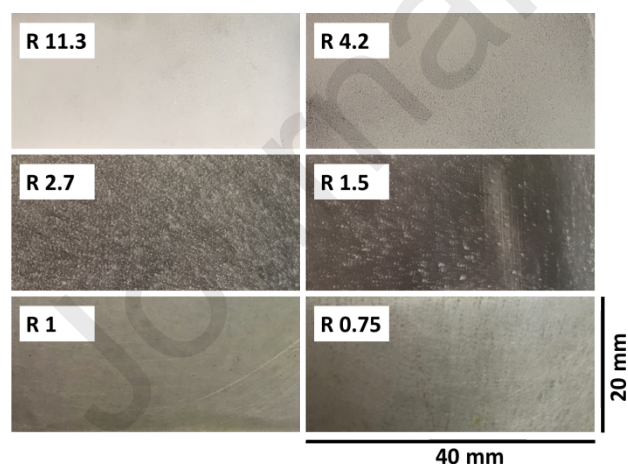


Figure 1: Pictures (from above) of the polyurethane films synthesized with castor oil and MDI at different NCO:OH ratios (abbreviated here as R) of 11.3, 4.2, 2.7, 1.5, 1 and 0.75. The temperature was 85°C. A tendency to a transparent polymer is seen with a decrease of NCO:OH ratio. White spots confirm the presence of excess NCO which did not react. All photographs are 40 mm by 20 mm and pictured on a stainless-steel background.

The second series of tests aimed to determine the feasibility of producing polyurethane from the different fractions of pyrolysis bio-oil at 75°C. The prepared films of polyurethane are shown in Figure 2 and the results are summarised in Table 2. The polyurethane of the whole bio-oil and the water soluble fraction were ineffective as polyols, presumably due to their low hydroxyl number. The ether-insoluble fraction produced a high quality polyurethane, due to the existence of phenols and other small polyols in this fraction. However, the ether insoluble fraction comprises < 2 wt.% of the bio-oil used here, meaning it is not viable economically as the main feedstock for producing a polyurethane from bio-oil. A uniform polyurethane was achieved using pyrolytic lignin (86 wt.%) at an NCO:OH ratio of 1 (Figure 2e). However the polymer became brittle when dried. The cross-linking number for this polymer was 0.94 ± 0.02 , so the brittleness likely results from the high degree of cross-linking. Adding pyrolytic lignin to MDI gradually resulted in a lower cross-linking number of 0.90 ± 0.01 . The resulting polyurethane was smooth and remained stable when dried (Figure 2f), as desired. Polyols such as castor oil are sometimes used to improve the properties of polyurethanes produced from other lignin sources. Here, we find castor oil had limited benefit in improving the properties of the resulting polymer, partly due to the poor miscibility of castor oil and the pyrolytic lignin. Finally we note that at NCO:OH ratios greater than 1, the resulting polyurethane was brittle, consistent with the observations when using castor oil. This finding suggests that all OH groups in the pyrolytic lignin were available for reaction, in contrast to previous work using kraft or organosolv lignin as a polyol, where only a portion of the hydroxyl groups in the lignin were available [33], [36], [38].

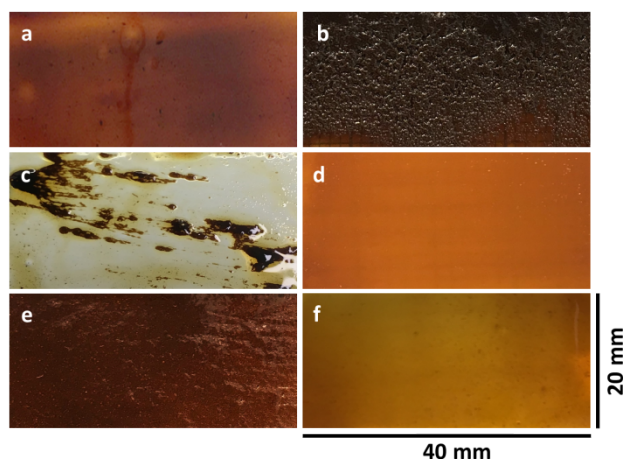


Figure 2: Pictures (from above) of polyurethane films of bio-oil and its fractions with MDI. a) A smooth film produced using whole bio-oil before drying. b) The film shown in a after drying. c) A polyurethane produced from WSF of bio-oil showing poor miscibility d) A polyurethane produced from ESF of bio-oil after drying. e) A polyurethane produced from pyrolytic lignin (86 wt.%) using the one-shot method. f) A polyurethane produced from pyrolytic lignin (86 wt.%) using the gradual addition method. All photographs are 40 mm by 20 mm.

Table 2: Observation of prepared polyurethanes produced from different polyols, combinations and addition methods.

Polyol	Addition method	Observations			
		Reactive	Malleable	Stable	Miscible
Whole bio-oil (R 1)	one-shot	✓	×	×	✓
Water soluble fraction of bio-oil (WSF)	one-shot	×	×	×	×
Ether insoluble fraction of bio-oil (EIF) (R 1)	one-shot	✓	✓	✓	✓
Pyrolytic lignin (86%) (R 1)	one-shot	✓	×	×	✓
Pyrolytic lignin (86%) (R 1)	gradual	✓	✓	✓	✓
Castor oil (10%) and pyrolytic lignin (75%) (R 1)	gradual	✓	✓	✓	×
Castor oil (4%) and pyrolytic lignin (81%) (R 1)	gradual	✓	✓	✓	✓
Pyrolytic lignin pre-polymer (R 1.3)	gradual	✓	✓	✓	✓
Castor oil pre-polymer (R 1.3), balance pyrolytic lignin	gradual	✓	✓	✓	×
Castor oil pre-polymer (R 1.1), balance pyrolytic lignin	gradual	✓	✓	✓	✓

Note: In the Table, the NCO:OH ratio is denoted by R. The final NCO:OH ratio for prepolymers was 1, in these cases the stated ratio refers to the NCO:OH ratio of the prepolymer only. All compositions given are in weight %. Shaded rows indicate preparations with attractive physical properties

To illustrate the quality of the polyurethane films produced, Figure 3 shows sections of polyurethane film produced from (a) castor oil and MDI and (b) pyrolytic lignin and MDI, under microscope. In each case, the slide was cut using a scalpel and the polymer film was observed from the side under a microscope. The castor oil-based polyurethane is clear and transparent and was approximately 30 μm thick. The castor oil-based polyurethane film was easy to peel off the glass slide. The pyrolytic lignin polyurethane was approximately 40 μm thick and is opaque and nearly black. It sticks to the glass slide, and was difficult to remove. SEM images of the polymer films are also shown in Figure 3. In this case, the slides were not cut as the high resolution of SEM meant that the fine edge of the film could be observed directly. In both images, the glass is visible at the bottom of the image and a bright white line indicates the interface with the polyurethane film. At the edge of the slide, the polyurethane films are thin, approximately 5 μm thick for the castor oil and 1 μm thick for the pyrolytic lignin polyurethane. The film thickness increases further from the edge, especially for the pyrolytic lignin polyurethane as the film is curved on the edges. No significant defects were observed in either the castor oil or pyrolytic lignin films, even at $\times 1500$ magnification, which was the maximum measured.

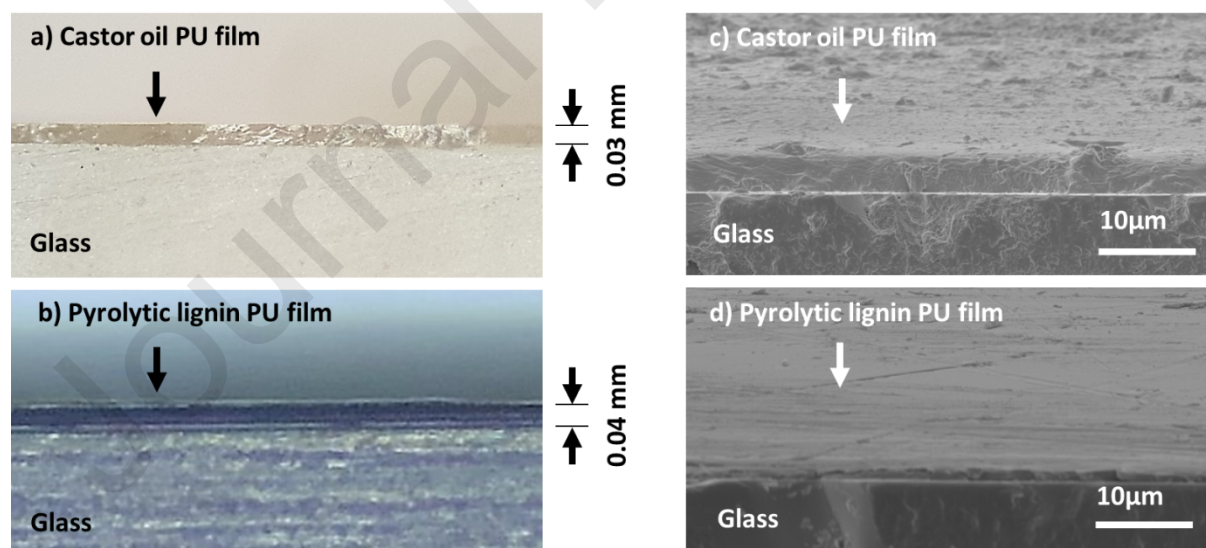


Figure 3: Examples of optical microscope images (a & b) and SEM images (c & d) of the polyurethane films produced from (a & c) castor oil and (b & d) pyrolytic lignin. In all cases, the polyurethane film was spread on a glass slide. The magnification of the SEM images was $\times 1500$.

In this section, polyurethane was produced from various components of the bio-oil. It was found that polyurethane films could be produced from pyrolytic lignin and the ether soluble fraction of bio-oil that were of high visual quality. The ether soluble fraction only comprises ~2 wt.% of the bio-oil, so pyrolytic lignin (32 wt.% of the bio-oil) is the most promising component of bio-oil from which to derive a polyurethane. The results demonstrate that it is possible to produce polyurethane films that appear to be of high quality visually, even when the bio-oil derived component is up to 86 wt.% of the polyurethane. The following sections will further characterise the produced polyurethane films.

3.2 Characterisation of polymers

3.2.1 Fourier Transform Infrared (FTIR) Spectroscopy

FTIR spectra for the bio-oil are expected to be complex. Therefore initially we examined FTIR spectra of castor oil-based polyurethanes as shown in Figure 4. The castor oil shows a broad peak between 3200 and 3600 cm^{-1} which corresponds to the OH group. The MDI has a strong peak at 2250 cm^{-1} , which is characteristic of the NCO functional group. The castor oil based polyurethane films show the NCO peak and the OH peak decreasing as the NCO:OH ratio approaches 1. In addition, a narrower peak centred at 3430 cm^{-1} is seen in all of the castor oil polyurethane films, which indicates the formation of the NH linkage of the polyurethane. The disappearance of the NCO and OH peak at NCO:OH ratios of ~1 confirms that all of the MDI reacts with the hydroxyl structures in the polyols. At NCO:OH ratios greater than 1, some of the NCO peak remains and indicates residual MDI is present, as expected. The formation of the urethane linkage is confirmed by the peaks at 1045 cm^{-1} and 1187 cm^{-1} , which are assigned to the ester C-O structures. The shoulder peak that appears at 1707 cm^{-1} , confirms a carbonyl structure is formed in the urethane linkage moiety. The peak at 1742 cm^{-1} in unreacted castor oil shifts to 1727 cm^{-1} in the polyurethane. This shift is ascribed to carbonyl stretching (C=O) [51]. The aromatic C-N peak (Ar-CN) in MDI at 1299 cm^{-1} shifts slightly to 1309 cm^{-1} in the polyurethane. These spectra illustrate the characteristic changes in the FTIR spectra when producing polyurethane from castor oil and MDI. Similar changes in the FTIR spectra are expected with the bio-oil-based polyurethane.

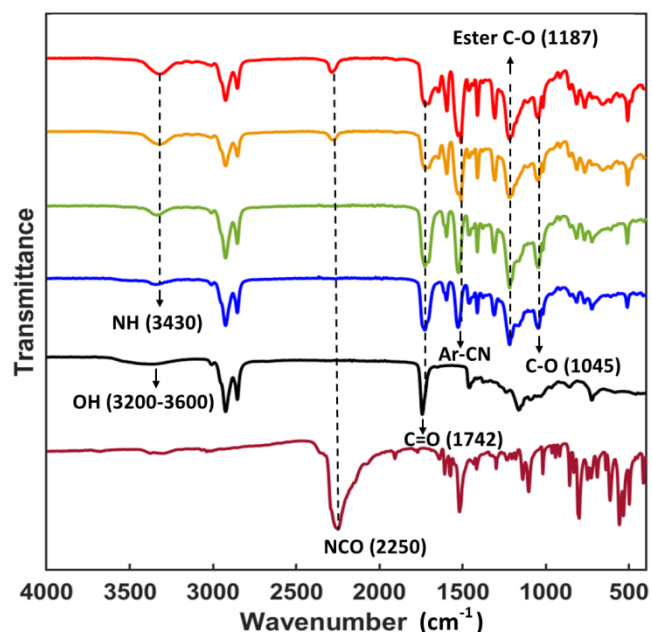


Figure 4: FTIR spectra of castor oil polyurethanes with NCO:OH ratios of (—) 1.5, (—) 1.25, (—) 1 and (—) 0.75 are illustrated. FTIR spectra are also shown for (—) castor oil and (—) MDI. Some of the key characteristic peaks are indicated in the figure. Consumption of MDI is confirmed by disappearance of the signal at 2250 cm^{-1} in the spectrum of polyurethanes. Formation of polyurethane linkages is characterised by C-O signals at 1045 and $1163\text{--}1210\text{ cm}^{-1}$. Another characterising feature is the shift of the broad OH signal ($3200\text{--}3600\text{ cm}^{-1}$) to a narrower signals centred at 3430 cm^{-1} in the polyurethane.

FTIR spectra of pyrolytic lignin, MDI and polyurethane films made from these are shown in Figure 5. The FTIR spectrum for pyrolytic lignin is significantly more complex and the peaks broader than that of castor oil, which makes identification of the changes in the chemical structure more challenging. However, the NCO linkage of MDI is still easily identified by the peak at 2250 cm^{-1} and this provides a key indicator of the consumption of MDI. Pyrolytic lignin also exhibits a broad peak at 3381 cm^{-1} that is characteristic of the hydroxyl groups. In the polyurethane films, the NCO peak at 2250 cm^{-1} disappears while the OH peak at 3381 cm^{-1} shifts slightly to 3321 cm^{-1} and also narrows. The shift of the OH peak is not as clear as it is with the castor oil polyurethane films, but can still be resolved. There is a wide range of chemicals in the bio-oil and thus it is likely that the NH peak in the bio-oil is associated with a variety of similar components, hence the resulting peak is less well defined. However, a higher transmittance at the position of the OH peak is observed as the NCO:OH ratio increases, confirming more consumption of OH groups. Furthermore, a peak

linked with the CO structure appears at 1187 cm^{-1} , which confirms the formation of the urethane linkage.

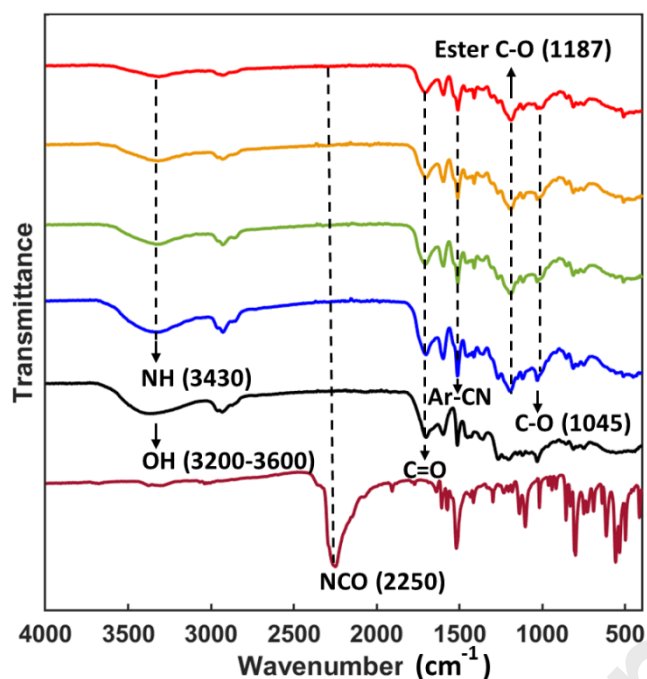


Figure 5: FTIR spectra of pyrolytic lignin polyurethanes with NCO:OH ratios of (—) 1.5, (—) 1.25, (—) 1 and (—) 0.75 are illustrated. FTIR spectra are also shown for (—) pyrolytic lignin and (—) MDI. Consumption of MDI is confirmed by the disappearance of the signal at 2250 cm^{-1} in the spectrum of polyurethanes. Formation of polyurethane linkages is characterised by C-O signals at 1187. Another characterising feature is a slight narrowing shift of the broad OH signal ($3200\text{--}3600\text{ cm}^{-1}$).

Interestingly, the NCO peak is gone in all of the polyurethane films produced from pyrolytic lignin. By contrast, in the equivalent spectra for the polyurethane derived from castor oil, the residual NCO is clearly visible if the NCO:OH ratio exceeds 1. It is hypothesised that the disappearance of the NCO is due to a reaction with another functional group in pyrolytic lignin that is not as readily reactive as the hydroxyl groups. To test this, FTIR spectra were acquired for a pyrolytic lignin polyurethane produced with an NCO:OH ratio of 1.5. Spectra were measured 24 h after producing polyurethane, however, in this case measurements were performed both before and after curing the polyurethane at 110°C for 4 h, see Figure 6. The peak at 2250 cm^{-1} which corresponds to the NCO structure of MDI, is still visible in the FTIR spectrum of the sample prior

to curing, albeit at a very low intensity. This observation confirms the existence of excess MDI when the polyurethane is not cured. The absence of the peak at 2250 cm^{-1} in the cured sample indicates that MDI is lost when the polyurethane is cured. The castor oil-based polyurethane films were also cured using the same process and the residual NCO was still visible in the FTIR spectra. Therefore, it is not the curing itself that causes the loss of the NCO peak. Instead it is hypothesised that the NCO reacts with some other component of pyrolytic lignin, in addition to the OH groups. This reaction proceeds more slowly than the reaction with the OH groups and hence does not appear to interfere with the formation of the polyurethane.

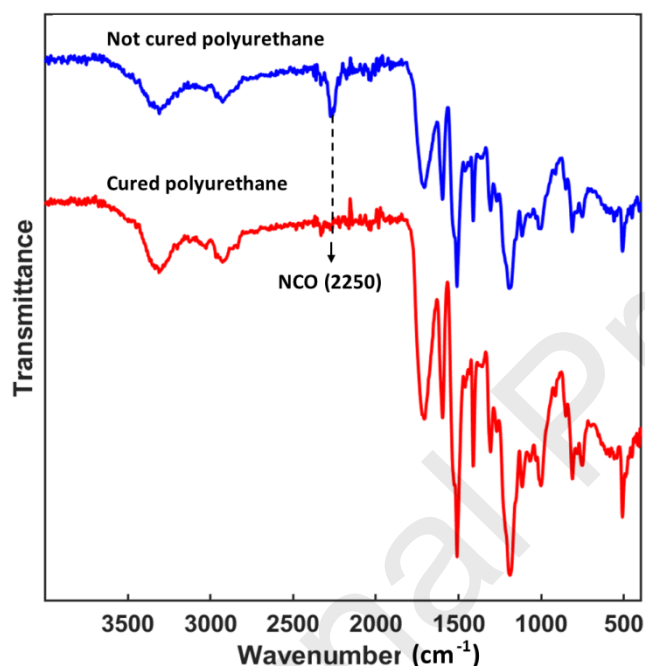


Figure 6: FTIR spectra of (—) pyrolytic lignin polyurethane that was not cured and (—) pyrolytic lignin polyurethane that was cured at 110°C for 4 h both at NCO:OH ratio of 1.5. The peak at 2250 cm^{-1} (NCO) disappears completely after the polyurethane is cured. It confirms that excess MDI is lost when the polyurethane is cured.

For completeness, FTIR spectra were also acquired for polyurethane produced from pyrolytic lignin using both the gradual step and prepolymer methods, as well as with the addition of castor oil (all at an NCO:OH ratio of 1). The resulting spectra are shown in Figure 7. In all cases, the resulting spectra are similar, though the polyurethane produced with some castor oil shows slightly narrower peaks in places. Consumption of MDI is confirmed by the disappearance of the

signal at 2250 cm^{-1} in the spectrum of polyurethanes. The formation of polyurethane linkages is characterised by the formation of the CO peak at 1187 cm^{-1} . Another characterising feature is the shift of the wide OH signal ($3200\text{-}3600\text{ cm}^{-1}$) to the signals of polyurethanes centred at 3430 cm^{-1} . No difference is observed when the polyurethane is produced directly or from a pre-polymer. These results indicate that the pre-polymer approach resulted in the same conversion of monomers to produce polyurethane. The difference in the extent of cross-linking cannot be determined from these FTIR spectra.

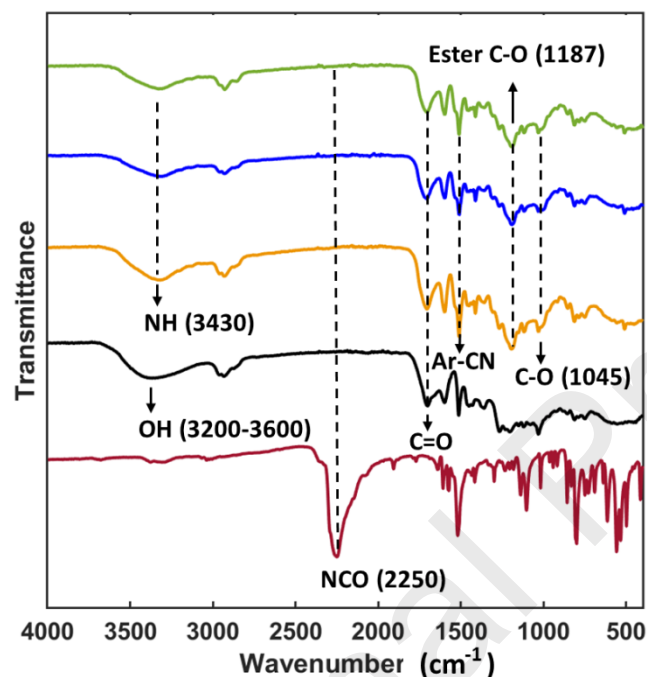


Figure 7: FTIR spectra are shown for pyrolytic lignin polyurethanes with NCO:OH ratio of 1 produced in one gradual step (—) and using a pyrolytic lignin pre-polymer approach with (—) pyrolytic lignin and (—) castor oil. The spectra of (—) pyrolytic lignin and (—) MDI are also included.

3.2.2 Thermal gravimetric analysis (TGA)

The thermal stability of a polymer provides an indication of its physical stability. It also indicates the main type of linkages in it. Weight loss of polyurethanes as the temperature increased from 30 to 600°C at the rate of $5^{\circ}\text{C min}^{-1}$ is shown in Figure 8. The decomposition curve of

polyurethanes can be divided into three stages: a stable stage, a weight loss stage and a stable stage at the terminal weight.

The castor oil polyurethane shows no significant weight loss until 300°C. Urethane, which is a carbamate structure, begins to break down above 300°C at the C-N bond [51]–[54]. The breaking of these structures continues until 360°C, when the decomposition rate slows. There is an increase in the rate of weight loss again at 380°C, where the thermal decomposition of the aliphatic chains (C-C) begins. At even higher temperatures the C-O and N-H bonds begin to fail. Aromatic structures begin to break above 480°C [5]. These bonds continue to break, along with C-H until 530°C [54]. The final residue for castor oil based polyurethane was approximately 16 wt.%. Similar TGA curves have been measured previously for polyurethane derived from castor oil, and other polyols [51]–[54].

Polyurethane films prepared from pyrolytic lignin begin to show significant weight loss above 160°C. The rate of weight loss of pyrolytic lignin decreased above 300°C, but then increases again from about 360°C, likely due to the degradation of the urethane linkage. The final residue consisted of approximately 50 wt.% of the pyrolytic lignin polyurethane. The pyrolysis of lignin is typically only significant at temperatures above 500°C due to the strong structure of lignin [55]. Therefore, polyurethane made of bio-oil can benefit from the stable structure of lignin at high temperatures. It is not clear why the initial rate of mass loss for the pyrolytic lignin polyurethane is greater than for the castor oil based polyurethane. It has previously been stated that a high OH number produces a high thermal stability in the resulting polyurethane [56]. The OH number of castor oil is 163 ± 3 mg KOH/g sample, compared with 70 ± 3 mg KOH/g sample for pyrolytic lignin. Therefore, the initial rate of weight loss may be linked to the low OH number of pyrolytic lignin. However, it is also likely that the initial weight loss of pyrolytic lignin polyurethane is due to the evaporation of filler chemicals present in pyrolytic lignin that did not react during the polymerisation.

TGA measurements were also performed on polyurethane prepared using the pre-polymer method, also shown in Figure 8. The weight loss of pre-polymer-based polyurethane films is initially similar to that of polyurethane produced using a single gradual addition. For

temperatures above 300°C the pre-polymer based polyurethane films show significantly greater weight loss. It is possible that the use of the pre-polymer may produce less cross-linking and hence slightly reduce the thermal stability of the polymer. However, the measured degree of cross-linking for both polyurethanes was approximately the same (0.90 ± 0.01 for the polyurethane produced using a single gradual addition and 0.89 ± 0.01 for the pre-polymer based polyurethane). Hence the reason for the decreased thermal stability of the prepolymer based polyurethane is unknown.

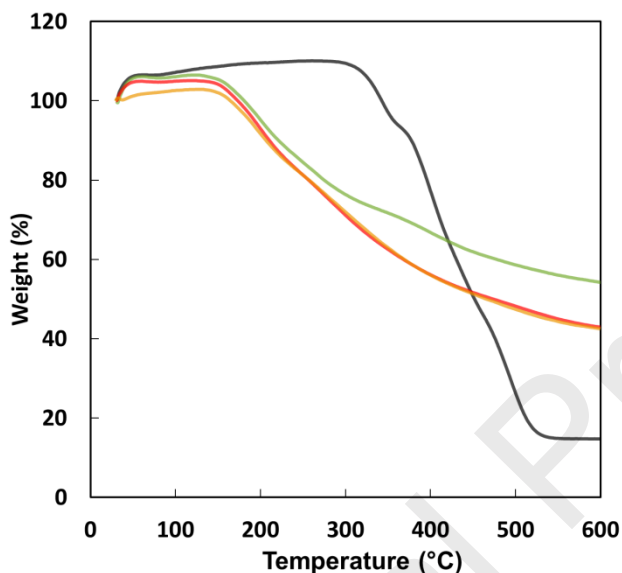
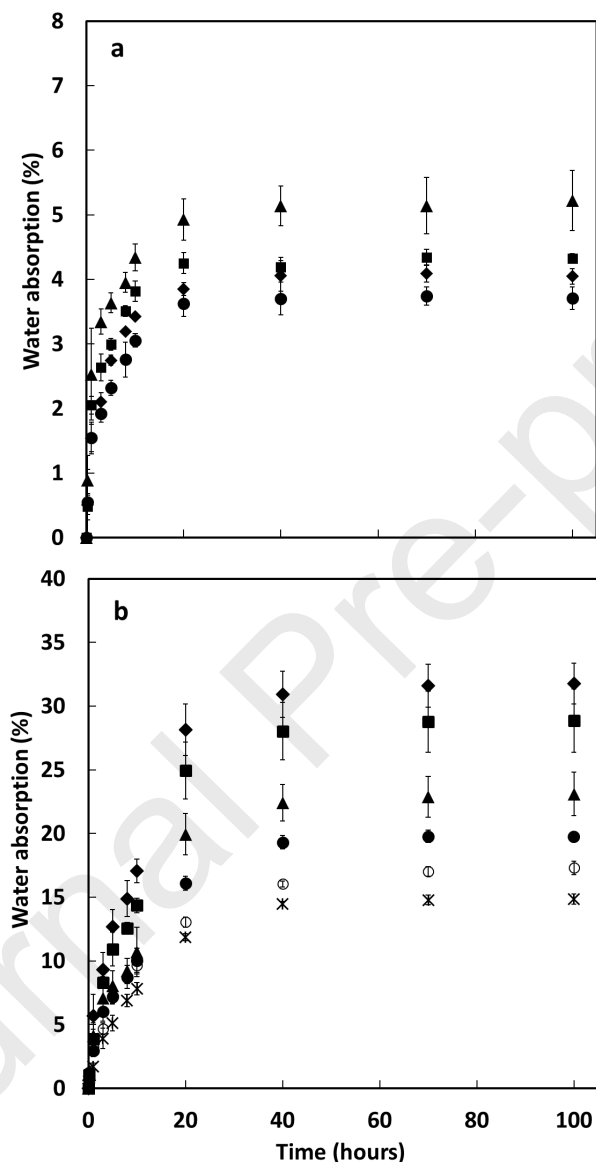


Figure 8: TGA curves of polyurethanes at an NCO:OH ratio of 1 including (—) castor oil polyurethane, (—) pyrolytic lignin polyurethane, and pre-polymer-based polyurethanes at NCO:OH ratio of 1, including (—) pyrolytic lignin polyurethane from pyrolytic lignin pre-polymer and (—) castor oil polyurethane from pyrolytic lignin pre-polymer are illustrated. Significant weight loss is observed for pyrolytic lignin polyurethanes from 150°C, whereas it is only observed for castor oil based polyurethanes from 300°C.

3.2.3 Water absorption

Polyurethane films are often used in situations where the absorption of water must be controlled. The water absorption of polyurethane films produced from castor oil and pyrolytic



lignin are shown in

Figure 9. In all cases, the water absorption approaches a constant value following an approximately exponential curve. The minimum water absorption occurs for an NCO:OH ratio of 1 for both castor oil- and pyrolytic lignin-based polyurethanes. The final water uptake in polyurethane films derived from castor oil was < 5 wt.%. The final water uptake in polyurethane films derived from pyrolytic lignin was between 15 and 30 wt.%. High water absorption typically

arises from either the hydrophilic nature of the polyol [57], or an open polymer structure. Castor oil includes 90% ricinoleic acid which is hydrophobic [58] and has a relatively simple molecular structure. Therefore it is unlikely that castor oil produces a complex pore network, nor is the resulting polyurethane likely to be hydrophilic. Hence, the low water absorption that was observed for the castor oil based polyurethanes was expected. The pyrolytic lignin fraction may contain species in addition to lignin, however, by definition the pyrolytic lignin fraction is all relatively insoluble in water and it is therefore unlikely that the resulting polyurethane film is hydrophilic. Instead it is hypothesised that the 3D structure of lignin and the consequent amorphous network may produce very fine cavities in the polymer [59], which increase the water uptake. This hypothesis is partially supported by the fact that final water uptake reduced in pre-polymer-based polyurethanes, in which cross-linking was marginally reduced.

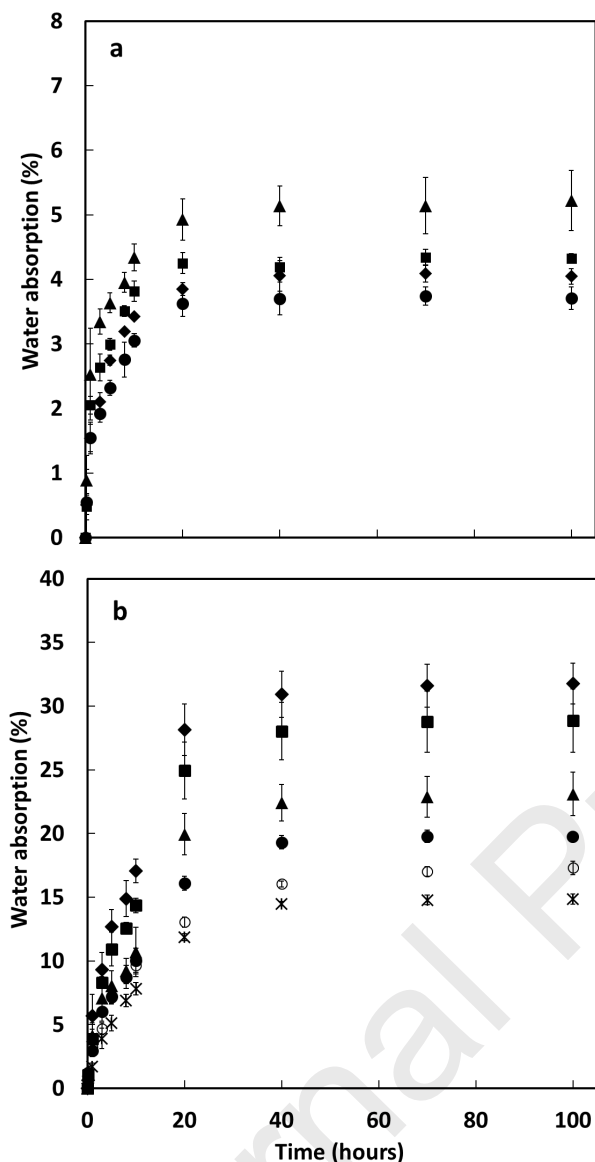


Figure 9: a) Water absorption of castor oil polyurethanes at NCO:OH ratios of (▲)0.75, (●)1, (■)1.25 and (◆)1.5 are illustrated. b) Water absorption of pyrolytic lignin polyurethanes at NCO:OH ratios of (▲)0.75, (●)1, (■)1.25 and (◆)1.5 and pre-polymer-based polyurethanes at NCO:OH ratio of 1 including (○) pyrolytic lignin polyurethane from pyrolytic lignin pre-polymer and (×) castor oil polyurethane from pyrolytic lignin pre-polymer are illustrated. Pyrolytic lignin polyurethanes show higher water absorption than castor oil polyurethanes. The pre-polymer approach has reduced water uptake. Note, the y-axes scales do not cover the same range.

The mechanism of water absorption can differ depending on, e.g., the chemical structure, or morphology [60]. The relationship between the water absorption ($\frac{m}{m_{\max}}$) and time (t) can be used

to infer the mechanism of water absorption by considering the initial period of time only. Assuming that the water absorption process can be expressed by Fickian diffusion, the absorption will follow an exponential model for short times (See Appendix).

Therefore, the relationship can be deduced by plotting $\log \frac{m}{m_{\max}}$ and $\log t$ for short times:

$$\log \frac{m}{m_{\max}} = \log a + n \log t \quad (4)$$

If the logarithmic plot of the mass fraction of water absorbed is linear and the slope n is close to 0.5, the absorption follows a Fickian model and the diffusion coefficient (D) can be calculated from a as follows:

$$\log a = \log \left(\frac{4D}{\pi h^2} \right)^{1/2} \quad (5)$$

Figure 10 shows a plot of $\frac{m}{m_{\max}}$ versus t for various polyurethane films at NCO:OH ratios of 1. The data are approximately linear on the logarithmic scale. The coefficients for these fits are given in Table 3. Although there is significant uncertainty in the estimated slopes, it can be seen that in most cases the slope is somewhat close to 0.5, indicating that Fick's law is a fair approximation for the water penetration into the polyurethane film.

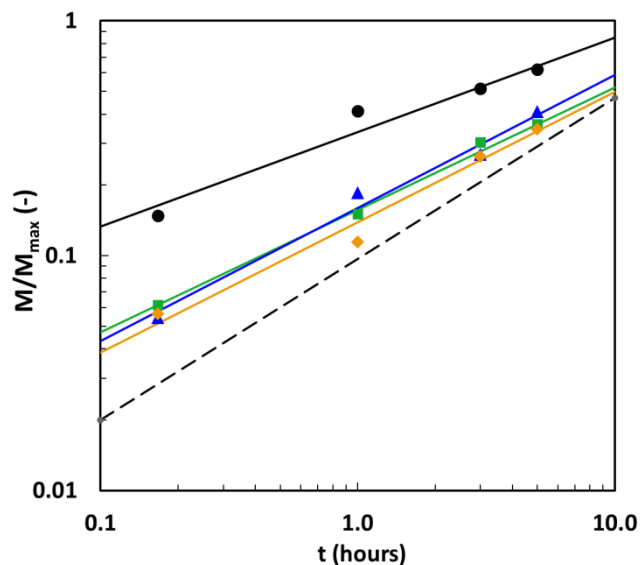


Figure 10 Water absorption of polyurethanes (all at NCO:OH ratio of 1) for (●) castor oil polyurethane, (●) pyrolytic lignin polyurethane, (●) pyrolytic lignin polyurethane from pyrolytic lignin pre-polymer and (●) castor oil polyurethane from pyrolytic lignin pre-polymer. The lines shown are fits of Eq 4 to the measured data, with each line colour coded to the associated measures data. A dashed line with a slope of 0.5 is added as an indication of the slope expected if Fick's law holds.

Table 3: Slopes of water absorption equations and the resulting diffusion coefficients for castor oil and pyrolytic lignin polyurethanes are listed.

Polyurethane	NCO:OH ratio	R ² value	<i>n</i>	<i>a</i>	<i>D</i> (10 ⁻⁹ m ² s ⁻¹)
Castor oil polyurethane	0.75	0.94	0.4 ± 0.1	0.38 ± 0.09	1.1 ± 0.5
	1.00	0.97	0.5 ± 0.2	0.30 ± 0.09	0.7 ± 0.4
	1.25	0.92	0.52 ± 0.06	0.32 ± 0.05	0.7 ± 0.2
	1.50	0.98	0.48 ± 0.02	0.31 ± 0.02	0.7 ± 0.2
Pyrolytic lignin polyurethane	0.75	0.98	0.48 ± 0.02	0.16 ± 0.01	0.3 ± 0.1
	1.00	0.99	0.52 ± 0.04	0.16 ± 0.01	0.3 ± 0.1
	1.25	0.97	0.68 ± 0.07	0.12 ± 0.02	0.2 ± 0.1
	1.50	0.91	0.81 ± 0.05	0.11 ± 0.01	0.17 ± 0.07
Castor oil polyurethane from pyrolytic lignin pre-polymer	1.00	0.99	0.60 ± 0.07	0.15 ± 0.03	0.2 ± 0.2
Pyrolytic lignin polyurethane from pyrolytic lignin pre-polymer	1.00	0.98	0.58 ± 0.04	0.13 ± 0.01	0.3 ± 0.1

Since the water absorption appears to follow a Fickian diffusion model, the diffusion coefficient for water penetrating into the polyurethane films for each sample was calculated. The thicknesses of the polyurethane films varied from 0.08 to 0.1 mm for the castor oil derived films

and from 0.1 to 0.15 mm for the pyrolytic lignin derived films. Therefore, the diffusion coefficient was estimated assuming average thicknesses of 0.09 ± 0.01 mm and 0.13 ± 0.03 mm for castor oil and pyrolytic lignin derived polyurethane films, respectively. Figure 11 shows the calculated diffusion coefficients for polyurethane derived from castor oil and pyrolytic lignin at different NCO:OH ratios. The uncertainty is estimated from the uncertainty in the fit of the parameter a , as well as the uncertainty in the thickness of the polymer film. The diffusion coefficients were all on the order of $10^{-10} \text{ m}^2 \text{ s}^{-1}$, and were lower for polyurethane derived from pyrolytic lignin than castor oil. The results also show that the diffusion coefficient decreases slightly as the NCO:OH ratio increases, though this effect is only marginal.

It is interesting to consider that the water absorption of the pyrolytic lignin derived polyurethane films was higher than for castor oil derived polyurethane films, while the diffusion coefficient for water to penetrate these films was lower for the pyrolytic lignin films. Slightly simplistically, it may be expected that the diffusion coefficient for water in a polymer film will be higher if the polymer is more hydrophilic. Hydrophilic polymers would also be expected to absorb more water. In this case, pyrolytic lignin absorbs more water but shows lower diffusivity, indicating that the high water absorption is not consistent with the polymer being more hydrophilic. This observation is also consistent with the fact that pyrolytic lignin is derived from components that are insoluble in water. Therefore, the low diffusivity, combined with the high water absorption may indicate that the pyrolytic lignin derived polyurethane films have an open microporous structure, with the passage between these micropores being slow and tortuous. However, there was no evidence of such porous network in the SEM images of the pyrolytic lignin derived polyurethane films, even at a magnification of 1500, indicating that if these pores are present and responsible for the water absorption and diffusivity, they must be very small. Further characterisation of the water transport through these polyurethane films is the subject of ongoing work.

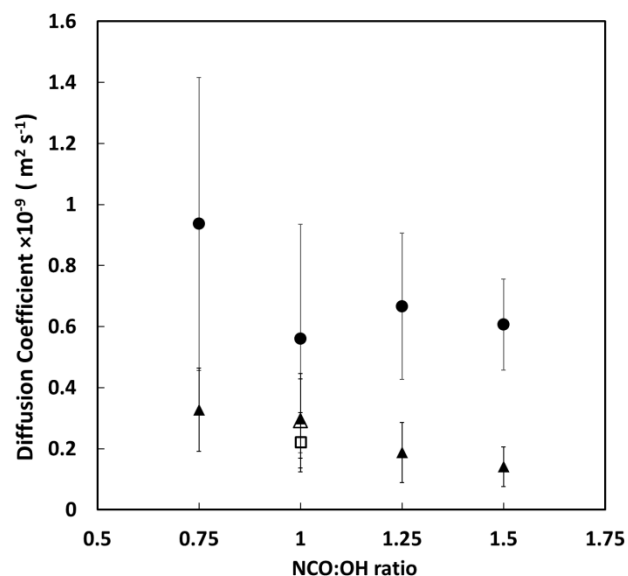


Figure 11: The effect of NCO:OH ratio on the diffusion coefficient is shown for (●) castor oil polyurethanes, (▲) pyrolytic lignin polyurethanes, (△) pyrolytic lignin polyurethane from pyrolytic lignin pre-polymer and (□) castor oil polyurethane from pyrolytic lignin pre-polymer. The diffusion coefficients were estimated from the water absorption data in Figure 10 assuming Fickian diffusion holds.

4 Conclusion

In this investigation, we demonstrate the possibility of manufacturing polyurethane with compounds extracted from pyrolysis bio-oil of woody biomass. The water-insoluble fraction was found to be the most suitable component of bio-oil to produce polyurethane due to the high proportion of it in the bio-oil and its suitability for producing polyurethane. This component is derived from lignin, so if used directly results in a brittle polymer, as previously reported for other lignin derived polyurethane films. Here, this issue has been overcome by adding pyrolytic lignin to MDI in a gradual manner. Using this method, it was possible to produce polyurethane with 86 wt.% pyrolytic lignin. A water absorption experiment revealed that this pyrolytic lignin derived polyurethane absorbed more water than a castor oil derived polyurethane. However, the diffusivity of water in pyrolytic lignin derived polyurethane was lower than for the castor oil derived polyurethane. These findings provide an important approach toward polymerisation of unmodified lignin.

5 Appendix

Assuming the water absorption follows a Fickian diffusion model, the molar flux of water through the surface of a film is given by [61]:

$$N_{x=0} = \left(\frac{D}{\pi t}\right)^{1/2} kC_0 \quad (6)$$

Where D is the diffusion coefficient, t is time, k is a partition coefficient, and C_0 denotes the initial concentration in contact with the surface.

The total mass of water in the film, m , is calculated by integrating Eq. 6 as follows:

$$m = AM \int_0^t \left(\frac{D}{\pi t}\right)^{1/2} kC_0 dt = 2kMC_0A \left(\frac{D}{\pi}\right)^{1/2} t^{1/2} \quad (7)$$

Where M is the molecular weight of water and A is the surface area.

The maximum water absorption m_{\max} in a film with a thickness of h is given by:

$$m_{\max} = kAC_0hM \quad (8)$$

Thus, the ratio of the water absorption at time t to the maximum water absorption gives:

$$\frac{m}{m_{\max}} = \left(\frac{4D}{\pi h^2}\right)^{1/2} t^{1/2} \quad (9)$$

Rearranging in logarithmic form gives:

$$\log\left(\frac{m}{m_{\max}}\right) = \log(a) + \frac{1}{2}\log t, \quad (10)$$

Where $a = \left(\frac{4D}{\pi h^2}\right)^{1/2}$. Therefore, the mass transfer behaviour can be examined by plotting $\frac{m}{m_{\max}}$ and t on a logarithmic scale for short times. If Fickian diffusion holds, the slope of the line will be one half (i.e. $\frac{1}{2}$). The diffusion coefficient is then calculated from a :

$$a = \left(\frac{4D}{\pi h^2} \right)^{1/2} \quad (11)$$

Silva et al. [62] derived a similar equation, except that there is a minor typographical error in the final formula.

6 Data availability

Data will be made available on request.

Journal Pre-proofs

References

- [1] A. Lee and Y. Deng, "Green polyurethane from lignin and soybean oil through non-isocyanate reactions," *Eur. Polym. J.*, vol. 63, pp. 67–73, 2015.
- [2] I. Banik and M. M. Sain, "Water blown soy polyol-based polyurethane foams of different rigidities," *J. Reinf. Plast. Compos.*, vol. 27, no. 4, pp. 357–373, 2008.
- [3] W. Lei, C. Fang, X. Zhou, Y. Cheng, R. Yang, and D. Liu, "Morphology and thermal properties of polyurethane elastomer based on representative structural chain extenders," *Thermochim. Acta*, vol. 653, no. April, pp. 116–125, 2017.
- [4] Trenkel, *Slow and controlled-release and stabilized fertilizers: an option for enhancing nutrient use efficiency in agriculture*, 2nd ed. Paris, 2010.
- [5] K. Mizera and J. Ryszkowska, "Polyurethane elastomers from polyols based on soybean oil with a different molar ratio," *Polym. Degrad. Stab.*, vol. 132, pp. 21–31, 2016.
- [6] X. Kong, L. Zhao, and J. M. Curtis, "Polyurethane nanocomposites incorporating biobased polyols and reinforced with a low fraction of cellulose nanocrystals," *Carbohydr. Polym.*, vol. 152, pp. 487–495, 2016.
- [7] M. Zieleniewska *et al.*, "Preparation and characterisation of rigid polyurethane foams using a rapeseed oil-based polyol," *Ind. Crops Prod.*, vol. 74, pp. 887–897, 2015.
- [8] X. Kong, G. Liu, H. Qi, and J. M. Curtisa, "Preparation and characterization of high-solid polyurethane coating systems based on vegetable oil derived polyols," *Prog. Org. Coatings*, vol. 76, pp. 1151–1160, 2013.
- [9] M. Kathalewar, A. Sabnis, and D. D'Melo, "Polyurethane coatings prepared from CNSL based polyols: Synthesis, characterization and properties," *Prog. Org. Coatings*, vol. 77, no. 3, pp. 616–626, 2014.
- [10] M. S. Gaikwad, V. V. Gite, P. P. Mahulikar, D. G. Hundiware, and O. S. Yemul, "Eco-friendly polyurethane coatings from cottonseed and karanja oil," *Prog. Org. Coatings*, vol. 86, pp. 164–172, 2015.
- [11] N. E. Marcovich, M. Kuranska, A. Prociak, E. Malewska, and K. Kulpa, "Open cell semi-rigid polyurethane foams synthesized using palm oil-based bio-polyol," *Ind. Crops Prod.*, vol. 102, pp. 88–96, 2017.
- [12] P. K. S. Pillai, S. Li, L. Bouzidi, and S. S. Narine, "Metathesized palm oil: fractionation strategies for improving functional properties of lipid-based polyols and derived polyurethane foams," *Ind. Crops Prod.*, vol. 84, pp. 273–283, 2016.
- [13] E. Reyhanitash, M. Tymchyshyn, Z. Yuan, K. Albion, G. Van Rossum, and C. Xu, "Hydrotreatment of fast pyrolysis oil: effects of esterification pre-treatment of the oil using alcohol at a small loading," *Fuel*, vol. 179, pp. 45–51, 2016.
- [14] J. Lehto, A. Oasmaa, Y. Solantausta, M. Kytö, and D. Chiaramonti, "Review of fuel oil

- quality and combustion of fast pyrolysis bio-oils from lignocellulosic biomass," *Appl. Energy*, vol. 116, pp. 178–190, 2014.
- [15] J. Lehto, A. Oasmaa, Y. Solantausta, M. Kytö, and D. Chiaramonti, "Fuel oil quality and combustion of fast pyrolysis bio-oils," *VTT Publ.*, vol. 116, no. 87, p. 79, 2013.
- [16] J. Piskorz and D. S. Scott, "Composition of oils obtained by the fast pyrolysis of different woods," *ACS Div. Fuel Chem. Prepr.*, vol. 32, no. 2, pp. 215–222, 1987.
- [17] B. J. Rashmi, D. Rusu, K. Prashantha, M. F. Lacrampe, and P. Krawczak, "Development of water blown bio-based thermoplastic polyurethane foams," *Adv. Mater. Res.*, vol. 584, no. October, pp. 361–365, 2012.
- [18] E. Hoekstra, S. R. A. Kersten, A. Tudos, D. Meier, and K. J. A. Hogendoorn, "Possibilities and pitfalls in analyzing (upgraded) pyrolysis oil by size exclusion chromatography (SEC)," *J. Anal. Appl. Pyrolysis*, vol. 91, no. 1, pp. 76–88, 2011.
- [19] A. Oasmaa, D. C. Elliott, and J. Korhonen, "Acidity of biomass fast pyrolysis bio-oils," *Energy and Fuels*, vol. 24, no. 12, pp. 6548–6554, 2010.
- [20] P. K. Kanaujia, Y. K. Sharma, M. O. Garg, D. Tripathi, and R. Singh, "Review of analytical strategies in the production and upgrading of bio-oils derived from lignocellulosic biomass," *J. Anal. Appl. Pyrolysis*, vol. 105, no. June, pp. 55–74, 2014.
- [21] R. H. Venderbosch, A. R. Ardiyanti, J. Wildschut, A. Oasmaa, and H. J. Heeres, "Stabilization of biomass-derived pyrolysis oils," *J. Chem. Technol. Biotechnol.*, vol. 85, no. 5, pp. 674–686, 2010.
- [22] A. Oasmaa, E. Kuoppala, A. Ardiyanti, R. H. Venderbosch, and H. J. Heeres, "Characterization of hydrotreated fast pyrolysis liquids," *Energy and Fuels*, vol. 24, no. 9, pp. 5264–5272, 2010.
- [23] C. Tessini *et al.*, "High performance thin layer chromatography determination of cellobiosan and levoglucosan in bio-oil obtained by fast pyrolysis of sawdust," *J. Chromatogr. A*, vol. 1218, no. 24, pp. 3811–3815, 2011.
- [24] Z. Hu, T. F. Yeh, H. M. Chang, Y. Matsumoto, and J. F. Kadla, "Elucidation of the structure of cellulolytic enzyme lignin," *Holzforschung*, vol. 60, no. 4, pp. 389–397, 2006.
- [25] M. Garcia-Perez, A. Chaala, H. Pakdel, D. Kretschmer, and C. Roy, "Characterization of bio-oils in chemical families," *Biomass and Bioenergy*, vol. 31, no. 4, pp. 222–242, 2007.
- [26] a. Oasmaa and E. Kuoppala, "Fast pyrolysis of forestry residue. 2. physicochemical composition of product liquid," *Energy & Fuels*, vol. 17, no. 7, pp. 1075–1084, 2003.
- [27] A. Oasmaa *et al.*, "Controlling the phase stability of biomass fast pyrolysis bio-oils," *Energy and Fuels*, vol. 29, no. 7, pp. 4373–4381, 2015.
- [28] R. J. M. Westerhof *et al.*, "Fractional condensation of biomass pyrolysis vapors," *Energy and Fuels*, vol. 25, no. 4, pp. 1817–1829, 2011.

- [29] F. Stankovikj and M. Garcia-Perez, "TG-FTIR method for the characterization of bio-oils in chemical families," *Energy and Fuels*, vol. 31, no. 2, pp. 1689–1701, 2017.
- [30] R. W. Thring, M. N. Vanderlaan, and S. L. Griffin, "Polyurethanes from Alcell® lignin," *Biomass and Bioenergy*, vol. 13, no. 3, pp. 125–132, Jan. 1997.
- [31] Y. Li and A. J. Ragauskas, "Ethanol organosolv lignin-based rigid polyurethane foam reinforced with cellulose nanowhiskers," *RSC Adv.*, vol. 2, no. 8, pp. 3347–3351, 2012.
- [32] J. P. S. Aniceto, I. Portugal, and C. M. Silva, "Biomass-based polyols through oxypropylation reaction," *ChemSusChem*, vol. 5, no. 8, pp. 1358–1368, 2012.
- [33] Y. Li and A. J. Ragauskas, "Kraft lignin-based rigid polyurethane foam," *J. Wood Chem. Technol.*, vol. 32, no. 3, pp. 210–224, 2012.
- [34] E. A. B. da Silva *et al.*, "An integrated process to produce vanillin and lignin-based polyurethanes from Kraft lignin," *Chem. Eng. Res. Des.*, vol. 87, no. 9, pp. 1276–1292, Sep. 2009.
- [35] J. Bernardini, P. Cinelli, I. Anguillesi, M. B. Coltelli, and A. Lazzeri, "Flexible polyurethane foams green production employing lignin or oxypropylated lignin," *Eur. Polym. J.*, vol. 64, pp. 147–156, 2015.
- [36] C. S. Carrico, T. Fraga, and V. M. D. Pasa, "Production and characterization of polyurethane foams from a simple mixture of castor oil, crude glycerol and untreated lignin as bio-based polyols," *Eur. Polym. J.*, vol. 85, pp. 53–61, 2016.
- [37] T. T. M. Tan, "Cardanol–lignin-based polyurethanes," *Polym. Int.*, vol. 41, no. 1, pp. 13–16, Sep. 1996.
- [38] X. Luo, Y. Xiao, Q. Wu, and J. Zeng, "Development of high-performance biodegradable rigid polyurethane foams using all bioresource-based polyols: lignin and soy oil-derived polyols," *Int. J. Biol. Macromol.*, vol. 115, pp. 786–791, 2018.
- [39] S.-P. Huo, M.-C. Nie, Z.-W. Kong, G.-M. Wu, and J. Chen, "Crosslinking kinetics of the formation of lignin-aminated polyol-based polyurethane foam," *J. Appl. Polym. Sci.*, vol. 125, no. 7, pp. 152–157, 2012.
- [40] S. Ilmiati, J. Hafiza, J. F. Fatriansyah, E. Kustiyah, and M. Chalid, "Synthesis and characterization of lignin-based polyurethane as a potential compatibilizer," *Indones. J. Chem.*, vol. 18, no. 3, pp. 390–396, 2018.
- [41] H. Hatakeyama, T. Kosugi, and T. Hatakeyama, "Thermal properties of lignin-and molasses-based polyurethane foams," *J. Therm. Anal. Calorim.*, no. 92, p. 419, 2008.
- [42] D. A. C. Evans, P. K. Annamalai, D. J. Martin, A. N. Hayati, and B. Laycock, "A simple methodology for improving the performance and sustainability of rigid polyurethane foam by incorporating industrial lignin," *Ind. Crops Prod.*, vol. 117, no. September 2017, pp. 149–158, 2018.

- [43] H. Yoshida, R. Mörck, K. P. Kringstad, and H. Hatakeyama, "Kraft lignin in polyurethanes I. Mechanical properties of polyurethanes from a kraft lignin–polyether triol–polymeric MDI system," *J. Appl. Polym. Sci.*, vol. 34, pp. 1187–1198, 1987.
- [44] G. Griffini, V. Passoni, R. Suriano, M. Levi, and S. Turri, "Polyurethane coatings based on chemically unmodified fractionated lignin," *ACS Sustain. Chem. Eng.*, vol. 3, no. 6, pp. 1145–1154, 2015.
- [45] A. Cornille, R. Auvergne, O. Figovsky, B. Boutevin, and S. Caillol, "A perspective approach to sustainable routes for non-isocyanate polyurethanes," *Eur. Polym. J.*, vol. 87, pp. 535–552, 2017.
- [46] M. Bil, J. Ryszkowska, P. Woźniak, K. J. Kurzydłowski, and M. Lewandowska-Szumieł, "Optimization of the structure of polyurethanes for bone tissue engineering applications," *Acta Biomater.*, vol. 6, no. 7, pp. 2501–2510, 2010.
- [47] M. A. Corcuera *et al.*, "Microstructure and properties of polyurethanes derived from castor oil," *Polym. Degrad. Stab.*, vol. 95, no. 11, pp. 2175–2184, 2010.
- [48] M. F. Abdul Patah, "Non-slugging entrained flow gasification of pyrolysis oil from radiata pine woody biomass," Univeristy of Canterbury, 2016.
- [49] J. Mitchell and D. M. Smith, *Aquametry: A treatise on methods for the determination of water (Chemical analysis) (Pt. 1)*. New York: Wiley, 1977.
- [50] ASTM Standard D4274, "Determination of hydroxyl numbers of polyols," *ASTM*, pp. 1–43, 2005.
- [51] M. E. V. Hormaiztegui, M. I. Aranguren, and V. L. Mucci, "Synthesis and characterization of a waterborne polyurethane made from castor oil and tartaric acid," *Eur. Polym. J.*, vol. 102, no. March, pp. 151–160, 2018.
- [52] V. L. Mucci, A. Ivdre, J. M. Buffa, U. Cabulis, P. M. Stefani, and M. I. Aranguren, "Composites made from a soybean oil biopolyurethane and cellulose nanocrystals," *Polym. Eng. Sci.*, vol. 58, no. 2, pp. 125–132, 2018.
- [53] J. Ferguson and Z. Petrovic, "Thermal stability of segmented polyurethanes," *Eur. Polym. J.*, vol. 12, no. 3, pp. 177–181, Jan. 1976.
- [54] P. N. Moghadam, M. Yarmohamadi, R. Hasanzadeh, and S. Nuri, "Preparation of polyurethane wood adhesives by polyols formulated with polyester polyols based on castor oil," *Int. J. Adhes. Adhes.*, vol. 68, pp. 273–282, 2016.
- [55] H. Yang, R. Yan, H. Chen, D. H. Lee, and C. Zheng, "Characteristics of hemicellulose, cellulose and lignin pyrolysis," *Fuel*, vol. 86, no. 12–13, pp. 1781–1788, 2007.
- [56] H. Liang, L. Liu, J. Lu, M. Chen, and C. Zhang, "Castor oil-based cationic waterborne polyurethane dispersions: Storage stability, thermo-physical properties and antibacterial properties," *Ind. Crops Prod.*, vol. 117, no. January, pp. 169–178, 2018.

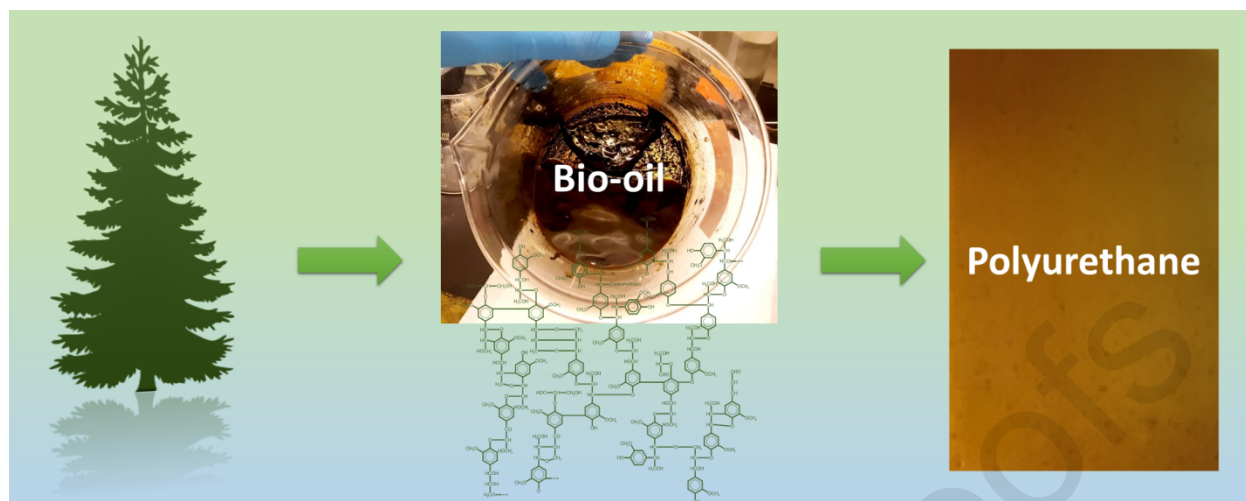
- [57] I. O. Bakare, F. E. Okieimen, C. Pavithran, H. P. S. Abdul Khalil, and M. Brahmakumar, "Mechanical and thermal properties of sisal fiber-reinforced rubber seed oil-based polyurethane composites," *Mater. Des.*, vol. 31, no. 9, pp. 4274–4280, Oct. 2010.
- [58] V. R. Patel, G. G. Dumancas, L. C. K. Viswanath, R. Maples, and B. J. J. Subong, "Castor oil: properties, uses, and optimization of processing parameters in commercial production," *Lipid Insights*, vol. 9, no. 1, pp. 1–12, 2016.
- [59] R. W. Thring, P. Ni, and S. M. Aharoni, "Molecular weight effects of the soft segment on the ultimate properties of lignin-derived polyurethanes," *Int. J. Polym. Mater. Polym. Biomater.*, vol. 53, no. 6, pp. 507–524, 2004.
- [60] S. K. Hosseinihashemi, F. Arwinfar, A. Najafi, G. Nemli, and N. Ayrilmis, "Long-term water absorption behavior of thermoplastic composites produced with thermally treated wood," *Meas. J. Int. Meas. Confed.*, vol. 86, pp. 202–208, 2016.
- [61] W. M. Dean, *Analysis of transport phenomena*, 2nd ed. New York: Oxford University Press, 1998.
- [62] L. Silva, S. Tognana, and W. Salgueiro, "Study of the water absorption and its influence on the Young's modulus in a commercial polyamide," *Polym. Test.*, vol. 32, no. 1, pp. 158–164, 2013.

Jaber Gharib: Writing - Original Draft, Methodology, Validation, Investigation **Shusheng Pang:** Resources, Writing – Review & Editing, **Daniel Holland:** Conceptualization, Writing – Review & Editing, Supervision

Declaration of interests

The authors declare that they have no known competing financial interests or personal relationships that could have appeared to influence the work reported in this paper.

The authors declare the following financial interests/personal relationships which may be considered as potential competing interests:



- Polyurethanes were synthesised from fractions of pyrolysis bio-oil
- Pyrolytic lignin was found to produce flexible polyurethanes
- Slow addition of pyrolytic lignin to the isocyanate was critical
- Resulting polyurethanes absorb 30wt% water, but show low diffusivity